Crystal structure and electrical properties of Ag₆PS₅I single crystal

I.P. Studenyak[1*], A.I. Pogodin[1], M.J. Filep[1, 2], O.P. Kokhan[1], O.I. Symkanych[1], M. Timko[3], P. Kopčanský[3]

[1]*Uzhhorod National University, 46, Pidhirna str., 88000 Uzhhorod, Ukraine*
[2]*Ferenc Rákóczi II Transcarpathian Hungarian Institute,*
Kossuth Sq. 6, Beregovo 90200, Ukraine
[3]*Institute of Experimental Physics, Slovak Academy of Sciences*
47, Watsonova str., 04001 Košice, Slovakia
*Corresponding author, e-mail: studenyak@dr.com

Abstract. The single crystals of quaternary halogen Ag_6PS_5I were grown from the solution–melt by means of a vertical zone crystallization method. The crystal structure has been ascertained using the Rietveld method. Investigation of electrical conductivity was carried out using the impedance spectroscopy technique within the frequency range $1 \cdot 10^1$–$3 \cdot 10^5$ Hz and temperature interval 293–383 K on gold contacts applied by chemical deposition from solution. Ionic ($1.79 \cdot 10^{-3}$ S/cm) and electronic ($1.64 \cdot 10^{-6}$ S/cm) components of electrical conductivity have been determined using the Nyquist plots. The mechanism of ionic conductivity for Ag_6PS_5I single crystal has been proposed which can be considered as ion diffusion through "channels" Ag2–Ag2.

Keywords: argyrodite, superionic conductor, single crystal, impedance spectroscopy, electrical conductivity, crystal structure.

1. Introduction

Secondary energy sources are becoming increasingly widespread in everyday life (portable electronic devices, electric vehicles, batteries) [1-3]. Currently, Li^+ ion batteries (LIB) with liquid electrolyte have received the greatest commercial use [1, 2, 4]. However, it should be noted that despite their widespread use, modern LIBs are approaching their limit of use and are not devoid of a number of shortcomings [1-3]. This leads to the search for new functional materials for energy storage, changes in the electrolyte material, *etc.* [1, 2]. One of the promising directions for the development of secondary energy sources is an all-solid-state battery (ASSB) with an inorganic solid-state ion conductor as an electrolyte [1, 2, 5].

Compounds related to solid-state ion conductors are characterized by significant ionic conductivity (due to mobile ions), a large number of possible crystallographic positions and their partial occupancy, polyhedra composition of crystal structure (provides the diffusion of ions) [6].

The above requirements are met by a wide class of ternary and quaternary compounds with the argyrodite structure [7-9]. These compounds contain two types of cations in their composition: 1) the multi-charge cation together with the anion forms a rigid anionic frame, 2) single-charge (rarely dual-charge) cation with different coordination and occupancy positions [7-9]. The most studied are phosphorus-containing argyrodites Me_7PS_6 and Me_6PS_5Hal (Me = Cu^+, Ag^+, Li^+; Hal = Cl, Br, I). For them, structural, electrical and optical properties were studied using the samples obtained in the form of single- and polycrystals, composites, ceramics and thin films [10-17].

Analysis of the available literature data indicates that the least studied is the compound Ag_6PS_5I, which was first described in the paper [7]. The authors of the paper [7] indicate that Ag_6PS_5I belong to cubic syngony ($F\bar{4}3m$, a = 10.474 Å), but their crystal structure is not described. The study of electrical conductivity of Ag_6PS_5I polycrystalline samples by using impedance spectroscopy in the frequency range of $2 – 20 \cdot 10^3$ Hz, the value of the total electrical conductivity ($1.2 \cdot 10^{-4}$ S/cm at 300 K) and the corresponding activation energy (0.24 eV) were determined. The higher value of electrical conductivity ($7.4 \cdot 10^{-4}$ S/cm at 300 K) and the lower value of activation energy (0.22 eV) for Ag_6PS_5I polycrystalline samples are given in the paper [18].

Electrical properties of composites based on $(Cu_{1-x}Ag_x)_6PS_5I$ solid solutions were investigated in Ref. [19].

The above mentioned defines the expediency of growing single crystals and detailed studies of Ag_6PS_5I crystal structure. Thus, the purposes of this work were as follows: to obtain Ag_6PS_5I in a single crystal form, study the peculiarities of crystal structure, measure ionic and electronic components of electrical conductivity, and ascertain the relationship between structural and electrical properties.

2. Experimental

Synthesis of Ag_6PS_5I was carried out in vacuumed down to 0.13 Pa silica ampoules by using simple substances: silver (99.995%), phosphorus (99.999%), sulfur (99.999%), and pre-synthesized binary silver (I) iodide, additionally purified using the directional crystallization method, taken in stoichiometric ratios. Ag_6PS_5I synthesis mode included a stepped heating up to 723 K at the rate close to 100 K/h (ageing during 48 h), a further increase in temperature up to 1100 K at the speed 50 K/h and ageing at this temperature for 24 hours. Cooling was performed in the oven off mode.
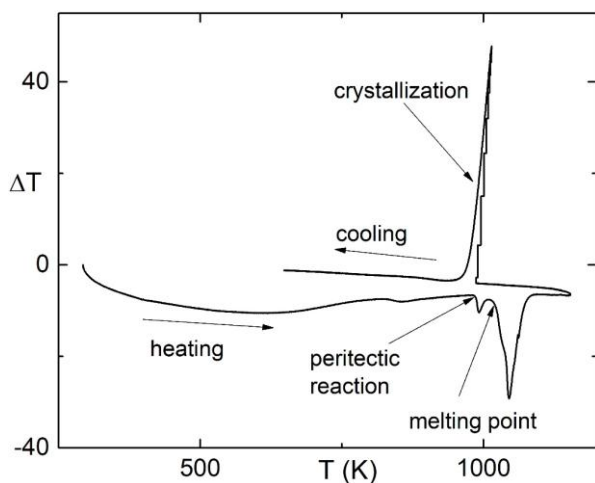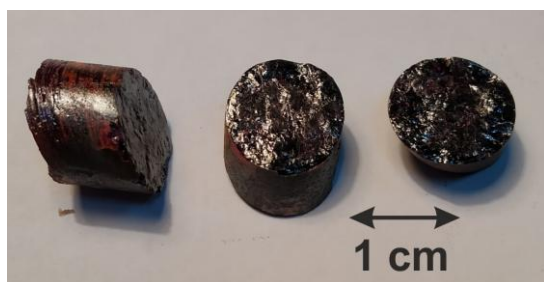

Fig. 1. Thermogram of Ag_6PS_5I compound.

Fig. 2. General view of Ag_6PS_5I single crystal.

To establish the optimal temperature regime for growing Ag_6PS_5I single crystals, studies were carried out by differential thermal analysis (Fig. 1) (chromel-alumel thermocouples, heating/cooling rate 700 K/h).

As can be seen from Fig. 1, two endothermic effects are observed on the thermogram in the heating mode at temperatures of 987 ± 5 K and 1023 ± 5 K. The first, obviously, corresponds to the peritectic decomposition reaction: $Ag_6PS_5I \leftrightarrow L + Ag_2S$, the second – liquidus. It should be noted that in the cooling mode there is only one exothermic effect (with hypothermia (1015 ± 5 K), which corresponds to formation of quaternary halogenchalcogenide: $L + Ag_2S \leftrightarrow Ag_6PS_5I$. Taking into account the nature of melting and crystallization, the growth of Ag_6PS_5I single crystals was carried out using the method of vertical zone crystallization from a solution–melt. The process took place in a two-zone tubular resistance furnace (melt zone temperature 1075 K, annealing zone – 680 K) using a special configuration silica container. In order to homogenize the melt, 24 hours of ampoule ageing was carried out in the melt zone. Growing the single crystal consists of formation of a seed in the lower conical portion of the container by applying the method of recrystallization in the course of 24 hours and the crystal build-up on the formed seed. The optimum rate of the crystallization front movement constituted 0.4…0.5 mm/h, the annealing temperature was 680 K (72 h), the cooling rate to room temperature –5 K/h. Using this method, Ag_6PS_5I single crystals of dark red colour with a metallic luster with the length of 30–40 mm and the diameter close to 12 mm were obtained (Fig. 2).

To study the peculiarities of crystal structure and to ascertain the mechanism of ionic conductivity, the study of obtained single crystal was carried out using X-ray analysis by the Rietveld method [20] (Fig. 3). The experimental data were obtained using the AXRD Benchtop powder diffractometer (Proto Manufacturing Limited) equipped with hybrid photon counting detector DECTRIS MYTHEN2R 1D, focusing geometry – Bragg–Brentano $\theta/2\theta$, CuKα radiation (Ni – filter), angle scanning range 10–120° 2θ with dynamic ROI (region of interest), exposition 1 s. Calculation and refinement of the model was carried out using the program EXPO 2014 [21], visualization – using VESTA 3.4.4 [22]. The main structural parameters of Ag_6PS_5I compound are given in Table.

Investigations of electrical conductivity of Ag_6PS_5I single crystal were carried out using impedance spectro-scopy [23] within the frequency range $1 \cdot 10^1 - 3 \cdot 10^5$ Hz and temperature interval 293–383 K with the high-precision LCR meter AT 2818. The amplitude of the alternating current constituted 10 mV. Measurement was carried out by the two-electrode method, on blocking (electronic) gold contacts. Gold contacts for measu-rements were applied by chemical precipitation from solutions. As starting solutions, 0.02M tetrachloroaurat (III) sodium Na[AuCl$_4$] and formalin solution (40% CH$_2$O+8% CH$_3$OH+52% H$_2$O) (deoxidant) were used in the ratio of 5/1 (selected experimentally).
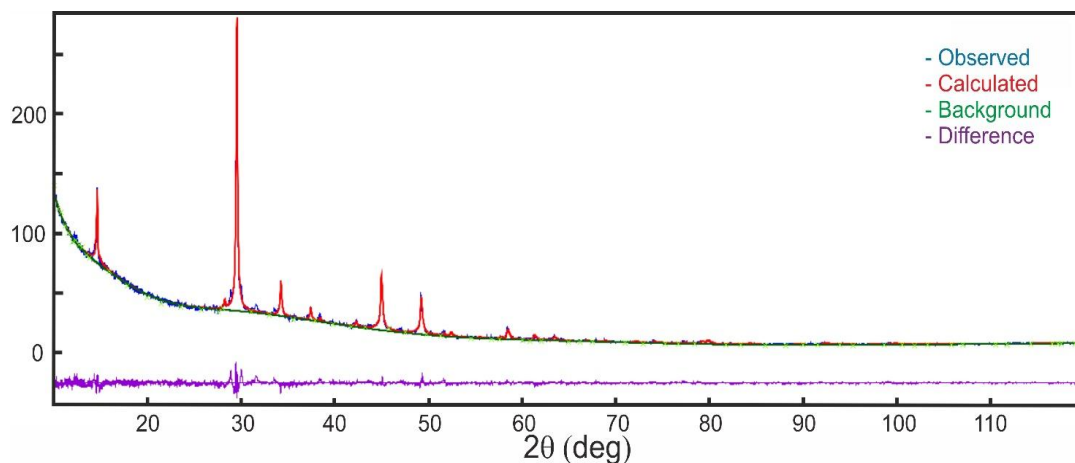
Studenyak I.P., Pogodin A.I., Filep M.J. et al. Crystal structure and electrical properties of Ag$_6$PS$_5$I ...

27

Fig. 3. Experimental and calculated diffractograms for Ag_6PS_5I. (Colour online.)

a)   b)
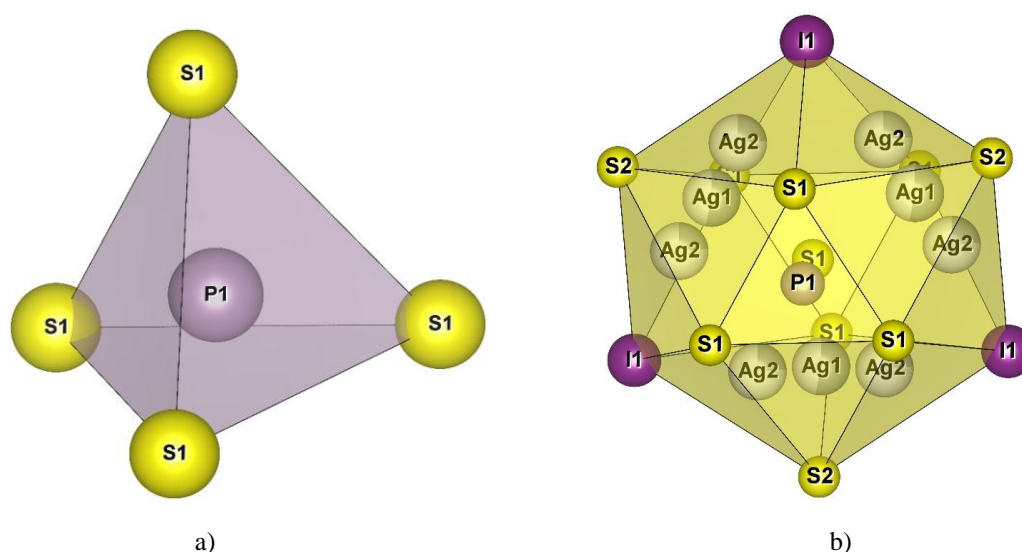
Fig. 4. [PS_4] tetrahedra (a) and [SS_9I_3] icosahedron (b) in the structure of Ag_6PS_5I.

Table. Parameters of crystal structure model for Ag_6PS_5I compound (positions, coordinates (*x, y, z*), isotropic atomic displacement parameters B_{iso}, and site occupancy factors (SOF); fixed value is marked with the asterisk *).

Atom	Position	x	y	z	B_{iso} (Å^2)	SOF
I1	4a	1.0000	0.5000	0.5000	4.147	1.000
S1	16e	1.1225	0.3775	0.1225	0.500*	1.000
S2	4d	0.7500	0.2500	0.2500	4.331	1.000
P1	4b	1.0000	0.5000	0.0000	4.941	1.000
Ag1	24g	0.9780	0.2500	0.2500	0.995	0.531
Ag2	48h	0.9707	0.3349	0.3349	0.674	0.239

Precipitation was carried out at the temperature no higher than 293 K. Increasing the temperature has a negative effect on the quality of deposited film due to the growth of recovery rate. The analysis of received dependences by using the Nyquist plots was carried out with the program ZView 3.5.

3. Results and discussion

3.1. Crystal structure

It is known that Ag_6PS_5I compound crystallizes in a face-centred cubic cell of argyrodite structure (spatial group $F\overline{4}3m$, $Z = 4$) with the lattice parameter $a = 10.4745(1)$ Å and is characterized by the presence of a rigid anionic frame and mobile cationic sublattice [7, 8]. The basis of the anionic frame of Ag_6PS_5I structure is [PS_4] (Fig. 4a), [S_3I] and [SI_4] tetrahedra, of which icosahedra are formed (Fig. 4b), which is typical for all compounds with argyrodite structure.

Studenyak I.P., Pogodin A.I., Filep M.J. et al. Crystal structure and electrical properties of Ag_6PS_5I ...
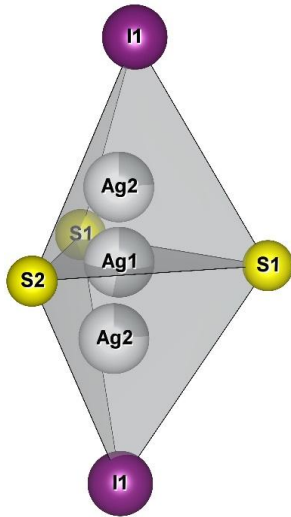
28

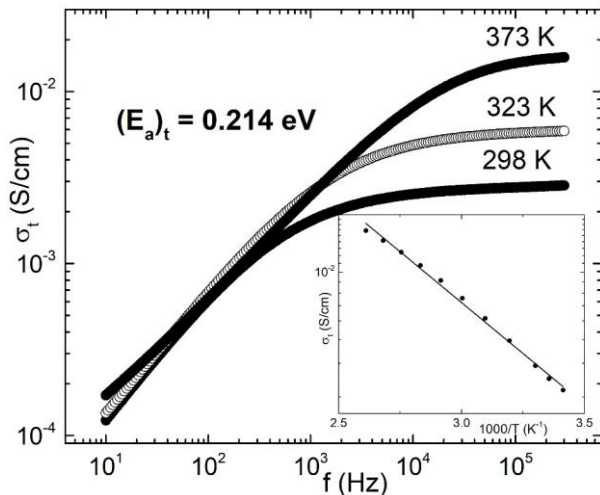**Fig. 5.** [S₃I₂] double tetrahedra in the structure of Ag₆PS₅I.

Fig. 6. Frequency dependences of total electrical conductivity at different temperatures for Ag₆PS₅I single crystal. The insert shows the temperature dependence of the total electrical conductivity at 100 kHz.

The icosahedra formed from the aforementioned tetrahedra are coordinated around the sulfur atom S1 (16e), which is simultaneously the vertex of [PS₄] tetrahedra. Since the presence of interpenetrating icosahedra is characteristic of the structure of the argyrodite, S1 is also the vertex of the next [SS₉I₃] icosahedron. In the structure of Ag₆PS₅I, [PS₄] tetrahedron (Fig. 4a) is symmetrical (absolutely central placement P), the lengths of P–S bonds are 2.222 Å, the distances S–S are 3.629 Å, the tetrahedron volume constitutes 5.63 Å³. Additionally, one can distinguish double tetrahedra [AgS₃I₂] (Fig. 5) formed by sulfur atoms S1, S2 and atom I1. These doubled polyhedra are coordinated around the Ag1 and Ag2 positions, from which a mobile cationic sublattice is formed.

Thus, in the structure of Ag₆PS₅I compound, two symmetrically independent silver atoms can be distinguished in the positions Ag1 (24g) and Ag2 (48h), with Ag1 being in triangular coordination of sulfur atoms (S1S2S1) with a slight displacement to the S1S2 edge, while the Ag2 atom is tetrahedrally coordinated (S1S2S1I1) with displacement to the planes of triangles (S1S2S1) and (S1S2I1) (Fig. 5).

3.2. Electrical conductivity

The frequency dependences of the total electrical conductivity at different temperatures for Ag₆PS₅I single crystal are shown in Fig. 6. With increasing the frequency, there is an increase in electrical conductivity, which is characteristic of materials with ionic conductivity in solid state [24]. In the insert to Fig. 6, the temperature dependence of the total conductivity at the frequency 100 kHz is shown. It is found that it is linear in nature and can be described by the Arrhenius equation, which testifies the thermoactivating character of conductivity. With its help, the activation energy of total electrical conductivity was determined, the value of which is in good agreement with the known literary data for Ag₆PS₅I [11, 18].

For a detailed analysis of the frequency behaviour of electrical conductivity, its separation into ionic and electronic components, the electrode equivalent circuit (EEC) and Nyquist plots were constructed [25]. It should be noted that the parasitic inductance of the cell ($\sim 2 \cdot 10^{-8}$ H) was taken into account during the analysis.

It was ascertained that Ag₆PS₅I single crystal possesses a rather low value of electronic conductivity ($\sigma_{ion} > \sigma_{el}$), which leads to the displacement of the low-frequency semicircle into the low-frequency region, which is the evidence of diffusion and relaxation processes influence. In the dependences $Z'–Z''$, two semicircles are observed in the entire temperature range (Fig. 7). The EEC selected for the description of the Nyquist plots can be separated into two parts: 1) ionic that includes elements describing the processes associated with the ionic component of conductivity, and 2) electronic that includes elements describing the processes associated with the electronic component of conductivity.

Diffusion relaxation processes at the boundary of electrode/crystal correspond to low-frequency semi-circles in the Nyquist plots, which is reflected by the included capacitance of the double diffusion layer C_{dl} (Fig. 7) with serially included elements R_{db}/C_{db}, which are responsible for the resistance and capacitance of the domain boundaries (the end of the low-frequency semicircle). The prevailing influence of diffusion and relaxation ion processes, against the background of sufficiently low specific values of electronic and ion components of electrical conductivity, leads to a fuzzy representation of high-frequency semicircles, which in turn are described by the processes of electrical conductivity of domains and represented in EEC by the serially connected resistance R_d (Fig. 7) with parallel-connected capacitance C_d.
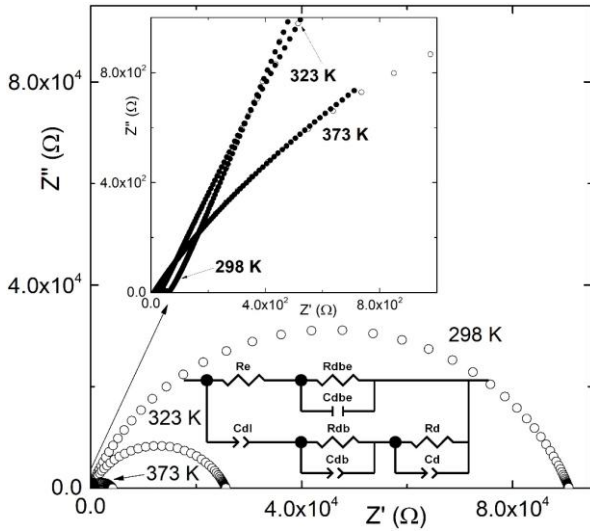
Studenyak I.P., Pogodin A.I., Filep M.J. et al. Crystal structure and electrical properties of Ag₆PS₅I ...

29

Fig. 7. EEC and Nyquist plots for Ag_6PS_5I single crystal at different temperatures. Experimental data correspond to the filled rings, calculated data – to the blank rings.

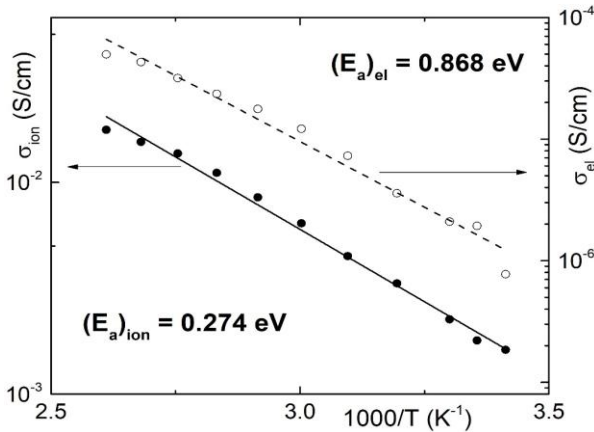**Fig. 8.** Temperature dependences of the ionic and electronic components of electrical conductivity for Ag_6PS_5I single crystal.

Thus, the ionic conductivity of Ag_6PS_5I single crystal is determined by the sum of the resistance of domain boundaries R_{db} and the resistance responsible for the electrical conductivity of the domains R_d. The nature of the domains of Ag_6PS_5I single crystal may be associated with the presence of a mosaic texture in the single crystal. In this case, the domain boundaries represent a structural heterogeneity, which manifests itself in the disorientation of texture elements <1° [26].

Parallel to the elements responsible for the ionic processes, EEC includes elements responsible for the electronic component of electrical conductivity, namely, the electronic resistance R_e and the electronic resistance of the domain boundaries R_{dbe} with the parallelly connected capacitance C_{dbe}, which contribute to the representation of both semicircles in the Nyquist plots. Consequently, the electronic component of electrical conductivity of Ag_6PS_5I is determined by the sum of the resistance of the domain boundaries R_{dbe} and the resistance R_e.

EEC presented in Fig. 7 describes the temperature behaviour of Ag_6PS_5I impedance in the entire temperature range under study, which is in good agreement with the description of ionic and electronic processes according to EEC. This is evidenced by the sequential degeneration of two semicircles into one observed at the temperature 373 K due to a significant decrease in contribution of the domain resistance R_d to the ionic conductivity.

The analysis of impedance spectra made it possible to investigate the temperature dependence of ionic and electronic components of electrical conductivity. It has been ascertained that they, like to the temperature dependence of the total electrical conductivity (insert to Fig. 6), have a linear character (Fig. 8) and are described by the Arrhenius law, which indicates the thermo-activation nature of conductivity. This allowed us to determine the activation energies of both ionic and electronic components of electrical conductivity.

Thus, the ionic conductivity of Ag_6PS_5I single crystal at 298 K is $1.79 \cdot 10^{-3}$ S/cm, whereas the value of the electronic component is $1.64 \cdot 10^{-6}$ S/cm.

3.3. Mechanism of ionic conductivity

Let us consider the mechanism of ion transport in the investigated Ag_6PS_5I compound. Although the Ag1 (24g) atom is located in the plane of the triangle S1S2S1, moving in the structure of Ag_6PS_5I is an atom in position Ag2 (48 h), which is shifted to the S1I1S2 plane and S2I edge. This is confirmed by the smaller value of SOF Ag2 (0.239) *vs.* Ag1 (0.531), and therefore the mechanism of ion transport can be considered as ion diffusion through "channels" Ag2–Ag2 (Fig. 9).

However, representative is the fact of a sufficiently low value of the ionic component of electrical conductivity in comparison with other Ag^+-conductive materials with the argyrodite structure, namely: crystals Ag_7GeS_5I and Ag_7SiS_5I, for which the ionic conductivity is $7.97 \cdot 10^{-3}$ S/cm [27] and $8.13 \cdot 10^{-3}$ S/cm [28], respectively. It should be noted that the ion transport for Ag_6PS_5I, based on the crystal structure, should be more efficient than for the aforementioned materials: SOF Ag2 – 0.239 (Ag_6PS_5I); 0.273 (Ag_7GeS_5I) [29]; 0.272 (Ag_7SiS_5I) [28], at maximum distances (d_{max}) (Ag2–Ag2) – 2.88 Å (Ag_6PS_5I); 3.09 Å (Ag_7GeS_5I); 2.79 Å (Ag_7SiS_5I). In this regard, let us consider the triangular pyramid Ag2S1S2 ($[AgS_3]$) (Fig. 10) that is a component of the doubled tetrahedron $[S_3I_2]$ (Fig. 5), which will allow estimating the displacement of the atom in position Ag2 relatively to the triangular plane S1S2 of the polyhedron $[S3I_2]$.

For quantitative analysis of the degree of Ag2 atom displacement relatively to the triangular plane S1S1S2, the parameters such as distortion index (*D*) and effective coordination number ECoN [22] are used. The distortion coefficient *D* is defined as the average value of the relative deviation of the lengths of bonds Ag–S in the above pyramid: $D = \dfrac{1}{n}\sum\limits_{i=1}^{n}\dfrac{|l_i - l_{av}|}{l_{av}}$, where l_i is the length of the individual bond, l_{av} – average bond length, and n –
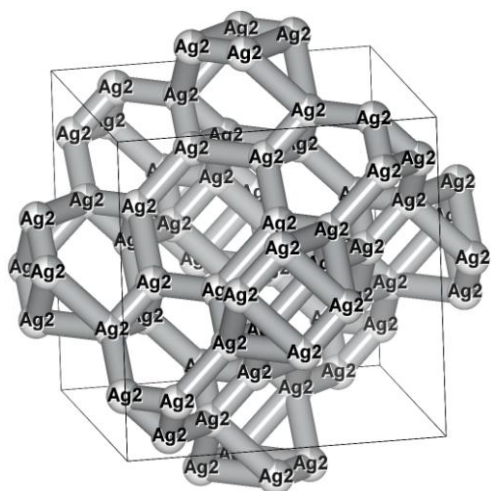
Studenyak I.P., Pogodin A.I., Filep M.J. et al. Crystal structure and electrical properties of Ag_6PS_5I ...

30

Fig. 9. Illustration of the mechanism of ion transport for Ag_6PS_5I compound on the example of "grid" of mobile cations migration at position Ag2.

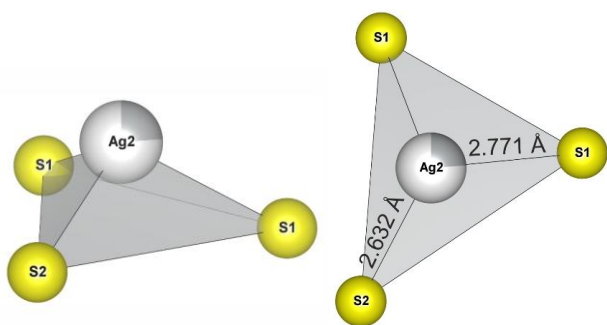**Fig. 10.** Triangular pyramid [AgS₃] in the structure of Ag_6PS_5I.

number of bonds in the polyhedron [22]. The content of ECoN parameter is defined as the sum of contributions of each bond to the effective coordination number:

$$\text{ECoN} = \sum_i \exp\left[1-\left(\frac{l_i}{l_{av}}\right)^6\right], \quad l_{av} = \frac{\sum_i l_i \exp\left[1-\left(\frac{l_i}{l_{min}}\right)^6\right]}{\sum_i \exp\left[1-\left(\frac{l_i}{l_{min}}\right)^6\right]},$$

where l_{min} is the minimum length of the bond. The contribution of each atom depends on the length of the bond and lies within the range from 0 to 1. If the distance between the central atom and the ligand atom increases, this number approaches to zero [22].

Calculation of the above parameters was carried out using the program VESTA 3 [22]. According to its results, it was found that in the compound Ag_6PS_5I the values of D and ECoN for Ag2 atom at the vertex of the triangular pyramid are 0.023 and 2.93, respectively. This indicates its almost central location relatively to the S1S1S2 plane and leads to a very slight displacement to the planes of triangles and edges [S₃I₂] of the double tetrahedron. For comparison, we give the values of D and ECoN for other aforementioned Ag^+ conductive materials: Ag_7GeS_5I (0.044; 2.66) and Ag_7SiS_5I (0.041; 2.72), which

ultimately indicates a stronger Ag2 displacement to the planes of triangles and edges [S₃I₂] of a double tetrahedron. On the other hand, it is known that triangular and linear coordination of cation are considered to be the most mobile positions in the structure of argyrodite. So, we can conclude that with other favourable parameters that allow evaluating the efficiency of ion transport, namely small values of SOF and d_{max}, the presence of a "closed" cation can be a determining limiting factor, which ultimately leads to strong reduction of ionic conductivity in this material.

4. Conclusions

The synthesis of quaternary halogenhalcogenide Ag_6PS_5I has been carried out, and the DTA method enabled to found that the compound has been formed in the course of a peritectic reaction. Dark red single crystals with the metallic luster as well as the length of 30–40 mm and diameter close to 12 mm are grown from the solution–melt by using the vertical zone crystallization method. The crystal structure of Ag_6PS_5I has been calculated using the Rietveld method, and the main structural parameters have been determined. The basic structural peculiarities of anionic and cationic sublattices on the example of structure-forming polyhedra have been found and discussed.

On the single-crystal Ag_6PS_5I sample, the total electrical conductivity has been measured using impedance spectroscopy within the frequency range from 10 Hz up to 300 kHz and temperature interval 293–383 K. Based on the frequency dependences of the total electrical conductivity, Nyquist plots have been constructed, which were further analyzed using electrode equivalent circuits. Using this approach, the total electrical conductivity has been separated into ionic and electronic components. This allowed us to obtain the numerical values of the ionic ($1.79 \cdot 10^{-3}$ S/cm) and electronic ($1.64 \cdot 10^{-6}$ S/cm) components of electrical conductivity, determine their ratio and activation energy of conductivities.

Comparison of the structural data and results of electrical measurements, in particular the values of ionic conductivity, has enabled to suggest and explain peculiarities of the mechanism of ion transport in the structure of Ag_6PS_5I, which can can be considered as ion diffusion through "channels" Ag2–Ag2.

References

1. Ohno S., Banik A., Dewald G.F. *et al.* Materials design of ionic conductors for solid state batteries. *Prog. Energy*. 2020. **2**. P. 022001. https://doi.org/10.1088/2516-1083/ab73dd.
2. Grey C.P., Hall D.S. Prospects for lithium-ion batteries and beyond – a 2030 vision. *Nat. Commun.* 2020. **11**. P. 6279. https://doi.org/10.1038/s41467-020-19991-4.
3. Duan J., Tang X., Dai H. *et al.* Building safe lithium-ion batteries for electric vehicles: a review. *Electrochem. Energ. Rev.* 2020. **3**. P. 1–42. https://doi.org/10.1007/s41918-019-00060-4.

Studenyak I.P., Pogodin A.I., Filep M.J. et al. Crystal structure and electrical properties of Ag_6PS_5I ...

31

4. Dubarry M., Baure G. Perspective on commercial Li-ion battery testing, best practices for simple and effective protocols. *Electronics*. 2020. **9**, No 1. P. 152. https://doi.org/10.3390/electronics9010152.

5. Sun Y.-K. Promising all-solid-state batteries for future electric vehicles. *ACS Energy Lett.* 2020. **5**, No 10. P. 3221–3223. https://doi.org/10.1021/acsenergylett.0c01977.

6. He X., Zhu Y., Mo Y. Origin of fast ion diffusion in super-ionic conductors. *Nat. Commun.* 2017. **8**. P. 15893. https://doi.org/10.1038/ncomms15893.

7. Kuhs W.F., Nitsche R., Scheunemann K. The argyrodites – a new family of tetrahedrally close-packed structures. *Mat. Res. Bull.* 1979. **14**, No 2. P. 241–248. https://doi.org/10.1016/0025-5408(79)90125-9.

8. Nilges T., Pfitzner A. A structural differentiation of quaternary copper argyrodites: Structure – property relations of high temperature ion conductors. *Z. Kristallogr.* 2005. **220**. P. 281–294. https://doi.org/10.1524/zkri.220.2.281.59142.

9. Zhou L., Assoud A., Zhang Q., Wu X., Nazar L.F. New Family of argyrodite thioantimonate lithium superionic conductors. *J. Am. Chem. Soc.* 2019. **141**, No 48, P. 19002–19013. https://doi.org/10.1021/jacs.9b08357.

10. Studenyak I.P., Stefanovich V.O., Kranjcec M. *et al.* Raman scattering studies of Cu_6PS_5Hal (Hal = Cl, Br, I) fast-ion conductors. *Solid State Ionics*. 1997. **95**. P. 221–225. https://doi.org/10.1016/S0167-2738(96)00477-8.

11. Beeken R.B., Garbe J.J., Gillis J.M. *et al.* Electrical conductivities of the Ag_6PS_5X and the Cu_6PSe_5X (X = Br, I) argyrodites. *J. Phys. Chem. Solids*. 2005. **66**, No 5. P. 882–886. https://doi.org/10.1016/j.jpcs.2004.10.010.

12. Pogodin A.I., Filep M.J., Malakhovska T.O. *et al.* The copper argyrodites $Cu_{7-n}PS_{6-n}Br_n$: Crystal growth, structures and ionic conductivity. *Solid State Ionics*. 2019. **341**. P. 115023. https://doi.org/10.1016/j.ssi.2019.115023.

13. Hanghofer I., Brinek M., Eisbacher S.L. *et al.* Substitutional disorder: structure and ion dynamics of the argyrodites Li_6PS_5Cl, Li_6PS_5Br and Li_6PS_5I. *Phys. Chem. Chem. Phys.* 2019. **21**, No 16. P. 8489–8507. http://doi.org/10.1039/C9CP00664H.

14. Orliukas A.F., Kazakevicius E., Kezionis A. *et al.* Preparation, electric conductivity and dielectrical properties of Cu_6PS_5I-based superionic composites. *Solid State Ionics*. 2009. **180**, No 2-3. P. 183–186. https://doi.org/10.1016/j.ssi.2008.12.005.

15. Studenyak I.P., Izai V.Yu., Studenyak V.I. *et al.* Influence of Cu_6PS_5I superionic nanoparticles on the dielectric properties of 6CB liquid crystal. *Liquid Crystals*. 2017. **44**, No 5. P. 897–903. https://doi.org/10.1080/02678292.2016.1254288.

16. Šalkus T., Kazakevičius E., Banys J. *et al.* Influence of grain size effect on electrical properties of Cu_6PS_5I superionic ceramics. *Solid State Ionics*. 2014. **262**. P. 597–600. https://doi.org/10.1016/j.ssi.2013.10.040.

17. Studenyak I.P., Kranjčec M., Izai V.Yu. *et al.* Structural and temperature-related disordering studies of Cu_6PS_5I amorphous thin films. *Thin Solid Films*. 2012. **520**, No 6. P. 1729–1733. https://doi.org/10.1016/j.tsf.2011.08.043.

18. Studenyak I.P., Kranjčec M. *Disordering Effects in Superionic Conductors with Adgyrodite Structure*. Uzhhorod: Hoverla, 2007 (in Ukrainian).

19. Studenyak I.P., Buchuk R.Yu, Bendak A.V. *et al.* Electric conductivity studies of composites based on $(Cu_{1-x}Ag_x)_6PS_5I$ superionic conductors. *SPQEO*. 2014. **17**, No 4. P. 425–428. https://doi.org/10.15407/spqeo17.04.425.

20. McCusker L.B., Von Dreele R.B., Cox D.E., Louër D., Scardi P. Rietveld refinement guidelines. *J. Appl. Crystallogr.* 1999. **32**, No 1. P. 36–50. https://doi.org/10.1107/S0021889898009856.

21. Altomare A., Cuocci C., Giacovazzo C. *et al.* EXPO2013: a kit of tools for phasing crystal structures from powder data. *J. Appl. Crystallogr.* 2013. **46**, No 4. P. 1231–1235. https://doi.org/10.1107/S0021889813013113.

22. Momma K., Izumi F. VESTA 3 for three-dimensional visualization of crystal, volumetric and morphology data. *J. Appl. Crystallogr.* 2011. **44**. P. 1272–1276. https://doi.org/10.1107/S0021889811038970.

23. Orazem M.E., Tribollet B. *Electrochemical Impedance Spectroscopy.* New Jersey: Wiley, 2008. https://doi.org/10.1002/9780470381588.

24. Ivanov-Schitz A.K., Murin I.V. *Solid State Ionics*. St.-Petersburg: Univ. Press, 2000 (in Russian).

25. Huggins R.A. Simple method to determine electronic and ionic components of the conductivity in mixed conductors a review. *Ionics*. 2002. **8**, No 3. P. 300–313. https://doi.org/10.1007/BF02376083.

26. West A.R. *Solid State Chemistry and its Applications*. Second Edition. Student Edition. John Wiley & Sons, Ltd, 2014.

27. Studenyak I.P., Pogodin A.I., Studenyak V.I. *et al.* Structure, electrical conductivity, and Raman spectra of $(Cu_{1-x}Ag_x)_7GeS_5I$ and $(Cu_{1-x}Ag_x)_7GeSe_5I$ mixed crystals. *Materials Research Bulletin*. 2021. **135**. P. 111116. https://doi.org/10.1016/j.materresbull.2020.111116.

28. Studenyak I.P., Pogodin A.I., Studenyak V.I. *et al.* Electrical properties of copper- and silver-containing superionic $(Cu_{1-x}Ag_x)_7SiS_5I$ mixed crystals with argyrodite structure. *Solid State Ionics*. 2020. **345**. P. 115183. https://doi.org/10.1016/j.ssi.2019.115183.

29. Studenyak I.P., Pogodin A.I., Kokhan O.P. *et al.* Crystal growth, structural and electrical properties of $(Cu_{1-x}Ag_x)_7GeS_5I$ superionic solid solutions. *Solid State Ionics*. 2019. **329**. P. 119–123. https://doi.org/10.1016/j.ssi.2018.11.020.

Studenyak I.P., Pogodin A.I., Filep M.J. et al. Crystal structure and electrical properties of Ag_6PS_5I ...

32

Authors and CV

Ihor P. Studenyak, defended his Dr. Sc. degree in Physics and Mathematics in 2003 and became full professor in 2004. Vice-rector for research at the Uzhhorod National University, Ukraine. Authored over 200 publications, 120 patents, 15 textbooks. The area of his scientific interests includes physical properties of semiconductors, ferroics and superionic conductors.

Artem I. Pogodin defended his PhD thesis in inorganic chemistry in 2016. Senior researcher at the Uzhhorod National University. Authored over 35 articles and 50 patents. The area of his scientific interests includes solid state chemistry, crystal growth, and materials science.
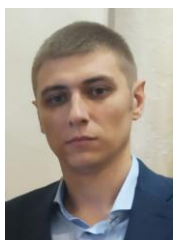
Mykhailo J. Filep, born in 1987, defended his PhD thesis in inorganic chemistry in 2015. Senior researcher at the Uzhhorod National University. Authored over 40 articles and 20 patents. The area of his scientific interests includes solid state chemistry and materials science.

Oleksandr P. Kokhan defended his PhD thesis in inorganic chemistry in 1996. Associate professor of Inorganic Chemistry Department at the Uzhhorod National University. Authored over 80 articles and 40 patents. The area of his scientific interests includes inorganic chemistry, solid state chemistry, crystal growth, materials science.

Olesya I. Symkanych defended her PhD thesis in the specialty "environmental safety" in 2016. Currently, she is associate professor of the Department of Ecology and Environmental Protection at the Uzhgorod National University. Author of 32 articles and 4 patents. Research interests: chemistry, chemical and radioecological monitoring, drug standardization.

Milan Timko, PhD in solid state physics. Senior researcher at the Institute of Experimental Physics, Slovak Academy of Science. Authored over 220 articles, 4 patents and 3 textbooks. The area of his scientific interests includes solid state physics, magnetic fluids and their magnetic, dielectric and hyperthermia properties.

Peter Kopčanský, Professor in solid state physics. Senior researcher at the Institute of Experimental Physics, Slovak Academy of Sciences. Authored over 250 articles, 6 patents, 5 textbooks. The area of his scientific interests: solid state physics, especially magnetism, transport properties in disordered systems, magnetic fluids, their magnetic and dielectric properties and composite systems with liquid crystals.

Кристалічна структура та електричні властивості монокристала Ag_6PS_5I

І.П. Студеняк, А.І. Погодін, М.Й. Філеп, О.П. Кохан, О.І. Симканич, М. Timko, P. Kopčanský

Анотація. Методом вертикальної зонної кристалізації з розчину–розплаву вирощено монокристали тетрарного галогенхалькогеніду Ag_6PS_5I. Кристалічну структуру встановлено з використанням методу Рітвельда. Дослідження електричної провідності проведено з використанням методу імпедансної спектроскопії в частотному діапазоні $1 \cdot 10^1 – 3 \cdot 10^5$ Гц та температурному інтервалі 293–383 K на золотих контактах, нанесених методом хімічного осадження з розчину. За допомогою діаграм Найквіста визначено іонну ($1.79 \cdot 10^{-3}$ S/cm) та електронну ($1.64 \cdot 10^{-6}$ S/cm) складові електричної провідності. Запропоновано механізм іонної провідності в суперіонному провіднику Ag_6PS_5I, який можна розглядати як дифузію іонів крізь «канали» Ag2–Ag2.

Ключові слова: аргіродит, суперіонний провідник, монокристал, імпедансна спектроскопія, електрична провідність, кристалічна структура.

Studenyak I.P., Pogodin A.I., Filep M.J. et al. Crystal structure and electrical properties of Ag_6PS_5I ...

33